Magnetic Resonance Imaging 61 (2019) 66–72

Contents lists available at ScienceDirect

Magnetic Resonance Imaging

journal homepage: www.elsevier.com/locate/mri

Original contribution

Role of diffusion weighted imaging and magnetic resonance spectroscopy in breast cancer patients with indeterminate dynamic contrast enhanced magnetic resonance imaging findings

Uma Sharma[a], Khushbu Agarwal[a], Smriti Hari[b], Sandeep R. Mathur[c], Vurthaluru Seenu[d], Rajinder Parshad[d], Naranamangalam R. Jagannathan[a,*]

[a] Departments of NMR & MRI Facility, All India Institute of Medical Sciences, New Delhi 110029, India
[b] Radio-diagnosis, All India Institute of Medical Sciences, New Delhi 110029, India
[c] Pathology, All India Institute of Medical Sciences, New Delhi 110029, India
[d] Surgical Disciplines, All India Institute of Medical Sciences, New Delhi 110029, India

ARTICLE INFO

Keywords:
Dynamic contrast enhanced MRI
Diffusion-weighted imaging
Magnetic resonance spectroscopy
Breast cancer
Apparent diffusion coefficient
tCho
Indeterminate DCE

ABSTRACT

Purpose: Dynamic contrast enhanced MRI (DCEMRI), diffusion weighted imaging (DWI) and in vivo proton (^{1}H) magnetic resonance spectroscopy (MRS) provides functional and molecular nature of breast cancer. This study evaluates the potential of the combination of three MR parameters [curve kinetics, apparent diffusion coefficient (ADC) and total choline (tCho) concentration] determined from these techniques in increasing the sensitivity of breast cancer detection.

Methods: MR investigations were carried out at 1.5 T on 56 patients with cytologically/histologically confirmed breast carcinoma. Single-voxel MRS was used to determine the tCho concentration. 3D FLASH was used for DCEMRI while single shot EPI based DWI was used for ADC determination.

Results: On DCEMRI, one patient showed type I curve, while 8 showed type II and 47 showed type III curve thus giving a sensitivity of 83.9% as detection rate of malignancy. tCho concentration was above cut-off value (2.54 mmol/kg) for 50/56 cases giving a sensitivity of 89.3%. Among 9 indeterminate DCEMRI cases, tCho showed malignancy in 6 cases with type II curve. DWI detected malignancy in 54/56 cases that included 9 cases that were false negative on DCEMRI, yielding a sensitivity of 96.4%. A total of 54 cases showed malignancy when any two of the three MR parameters was positive for malignancy yielding a sensitivity of 96.4% while it increased to 100% when any one parameters showed positive result.

Conclusion: DWI showed highest sensitivity of detection compared to DCEMRI and MRS. Multi-parametric approach yielded 96.4% and 100% sensitivity when any two or one of the three parameters was taken as positive for malignancy, respectively. Also the results demonstrated that addition of DWI and MRS play a significant role in establishing the final diagnosis of malignancy, especially in cases where DCEMRI is indeterminate.

1. Introduction

Breast cancer is a significant healthcare concern due to high mortality and morbidity associated with it, worldwide [1]. Early diagnosis of the disease is an essential step towards successful treatment and for increasing the survival rate of breast cancer patients. Dynamic contrast enhanced magnetic resonance imaging (DCEMRI) of breast has become a standard technique for diagnosis of breast lesions [2]. It has found important applications in the detection of mammographically occult lesions and in providing detailed morphological extent and kinetics of breast lesions. Combined use of both architectural and contrast enhanced kinetics features has significantly improved the diagnostic

Abbreviations: DCEMRI, dynamic contrast enhanced magnetic resonance imaging; MRS, magnetic resonance spectroscopy; DWI, diffusion weighted imaging; ADC, apparent diffusion coefficient; tCho, total choline; LABC, locally advanced breast cancer; DCIS, ductal carcinoma in situ; AJCC, American Joint Committee on Cancer; BIRADS, breast imaging reporting and data system; PRESS, point resolved spectroscopy; FLASH, fast low angle shot; ROI, region of interest; ER, estrogen receptor; PR, progesterone receptor; HER2-neu, human epidermal growth factor; FNAC, fine needle aspirate cytology; IHC, immuno-histochemistry; Gd-DTPA, gadolinium diethylene triamine penta acetic acid; SS-EPI, single shot echo planar imaging

* Corresponding author
E-mail address: jagan1954@hotmail.com (N.R. Jagannathan).

https://doi.org/10.1016/j.mri.2019.05.032
Received 2 February 2019; Received in revised form 20 May 2019; Accepted 21 May 2019

ability of DCEMRI [2]. However, there are limitations in its specificity due to overlap between morphological features and kinetics patterns of benign and malignant lesions [2,3].

Diffusion weighted imaging (DWI) is one of the recent additions in clinical MR workup. It provides information on diffusion of water molecules in the tissues, quantified as apparent diffusion coefficient (ADC) and has shown potential in characterizing breast lesions [4–6]. Several studies have documented that malignant lesions were characterized by lower ADC values in comparison to benign lesions [4–6] which was attributed to high cellularity of malignant tumors [7,8]. Studies have demonstrated that addition of DWI increased the specificity of DCEMRI [4,9–11] and the T2-weighted imaging [4,6]. However, the major limitation of DWI is that the small cancer foci may not clearly be seen on ADC maps [4,6,10,12].

Another MR technique, in-vivo magnetic resonance spectroscopy (MRS), offers unique information on the biochemical characteristics associated with the malignant transformation in a non-invasive manner [13–26]. The diagnostic ability of MRS is essentially based on the detection of increased levels of choline containing compounds (tCho) in malignant breast lesions which have been shown to differentiate them from benign lesions and augment the specificity of MRI [13–26]. Choline containing compounds such as phosphocholine and glycerophosphocholine serve as precursors of membrane phospholipids. Increased levels are attributed to increased membrane biosynthesis reflecting proliferation of tumors [15,27]. Quantitative estimate of the concentration of tCho using in vivo MRS and the cut-off values of tCho concentration in the differentiation of malignant from benign breast lesions have also been reported [19,20].

Though the role of various MR techniques has been evaluated in breast lesions, there are no well-defined guidelines for the use of various MR parameters (as standalone or in combination) for the diagnosis of breast lesions in a clinical setting. Recently, several studies documented that combination of two or three MR parameters like ADC, contrast kinetics features and tCho have exhibited potential of enhancing the diagnostic ability of MR based approach [25,26,28,29]. We have earlier briefly reported the role of ADC in characterizing the malignant breast lesions with indeterminate DCE findings [5]. In the present study, we included the results of ^{1}H MRS in these patients and retrospectively evaluated the role of multi-parametric approach of combining the data from DCEMRI, DWI and MRS in increasing the sensitivity of detection of breast lesions.

2. Material and methods

2.1. Patients and controls

A total of 56 women with cytologically/histopathologically proven locally advanced breast cancer [with stages IIB and III (A, B, & C)] attending the breast cancer clinic of our Institute were enrolled for this study during the period 2012–2016. All patients underwent all three MR examinations, DCEMRI, DWI and ^{1}H MRS and the data was retrospectively evaluated. The study was approved by the institute ethics committee and written informed consent was obtained from all patients. Patients were evaluated based on triple assessment criteria that comprised of physical examination, radiological examination (ultrasound/mammography) followed by pathological evaluation [fine needle aspiration cytology/core biopsy]. An experienced radiologist (SH) evaluated the mammography images and reported Breast imaging Reporting and Data System (BI-RADS) classification of lesions prior to MRI and histopathological evaluation. Malignancy was confirmed using histopathological evaluation of ultrasound guided/core needle biopsied tissue. Diagnosis of lesions was based on histopathology of core biopsy in 54 patients while in two patients cytology of fine needle aspirate was performed. Clinical staging of all lesions was in accordance with American Joint Committee on cancer (AJCC) tumor, node, and metastasis (TNM) staging criteria. Immuno-histochemical (IHC) examination of biopsied tissue was performed to determine the expression status of hormonal receptors like estrogen receptor (ER), progesterone receptor (PR) and human epidermal growth factor (HER2/neu). Metastatic workup included liver function tests, chest roentgenograms, ultrasound of the abdomen and pelvis and bone scan.

2.2. Inclusion and exclusion criteria

The inclusion criteria include patients with cytologically/histopathologically proven malignant lesions (with stage IIA, IIB and IIIA, IIIB + C). Patients with metastasis, atypia, claustrophobic, on prior treatment, radial scar, pregnant, using contraceptive pills, metallic implants, pacemaker, etc., and also those not willing to take part in the study, were excluded.

2.3. Magnetic resonance imaging (MRI) and dynamic contrast enhanced imaging (DCEMRI)

MR investigations were performed using a four channel phased array breast matrix receiver coil at 1.5 T (Magnetom AVANTO, Siemens Healthcare Sector, Germany). Patients were positioned in a head first prone position with both the breasts fitting into the cups of the double breast coil. Following the scout images, short tau inversion recovery coronal images were acquired with a TR and a TE of 6940 ms and 58 ms, respectively with a slice thickness of 3 mm and a matrix size of 320 × 256. Also, fat suppressed MR images were acquired in transverse and sagittal planes (TR and TE of 6270 and 102 ms; slice thickness = 3 mm with no gap; matrix size = 512 × 440). DCEMRI in the axial plane was carried out using a fat-saturated 3D FLASH sequence with the following parameters: TR and TE of 5.46 and 2.53 ms, respectively; flip angle = 12°; matrix size = 305 × 448; slice thickness = 1.4 mm with no gap. Gadolinium-diethylene triamine penta acetic acid (Gd-DTPA) contrast agent (0.1 mmol/kg) was injected using automatic injector at a rate of 2 ml/s followed by saline flush. One pre-followed by 5 post-gadolinium image series were acquired with a total acquisition time of 5.5 min (6 × 55 s).

2.3.1. Tumor volume calculation

The subtracted axial dynamic MR images (pre-contrast subtracted from post-contrast) were used for the measurement of tumor volumes. Tumor area was segmented manually slice-by-slice using free hand ROIs in all slices (no inter slice gap) in which the tumor was visualized by one of the authors (KA) under the guidance of an experienced radiologist (SH). Perimeter method was used for calculating the tumor volume: volume = ST ($A_1 + A_2 \ldots A_n$) here ST refer to the slice thickness and A_n the area of the tumor in n^{th} slice.

2.4. Diffusion weighted imaging (DWI)

DWI sequence was calibrated at 25 °C using single compartment phantoms of water and acetone. The mean ADC for water and acetone were 2.25 ± 0.03 × 10^{-3} mm^2/s and 4.1 ± 0.17 × 10^{-3} mm^2/s respectively and is in agreement with the earlier literature report [8]. Reproducibility of ADC measurements were checked with repeated measurements and the coefficient of variance calculated were within 1% and 4% of error limit for water and acetone, respectively. Diffusion weighted imaging was performed prior to DCEMRI. Multi-slice single shot echo planar imaging (SS-EPI) sequence was used to acquire DW images in the transverse plane covering both the breasts. The diffusion gradients were applied along the orthogonal direction concurrently to reduce motion artifacts. The parameters used for DWI were: b = 0, 500 and 1000 mm^2/s; TR = 5000 ms; TE = 87 ms; field of view (FOV) = 250–350 mm; number of averages = 1; EPI factor = 128; acquisition matrix = 128 × 128; and slice thickness = 4 to 5 mm without any inter slice gap. The total acquisition time was 42 s.

2.4.1. ADC measurements

ADC maps were constructed using the standard software provided by the manufacturer. Tumor region of interest (ROI) were manually delineated on a single slice with largest diameter on ADC map by one of the authors (KA) under the supervision of an experienced radiologist (SH). Care was taken to select areas that were hyperintense on DCEMR subtracted images (pre-contrast subtracted from post-contrast), and on DWMRI while hypointense on ADC maps. Multiple non-overlapping contiguous circular ROIs of five pixels each (size = 0.49 cm^2) were drawn manually on the hypointense areas covering the entire tumor region visualized on a single slice. However, care was taken to exclude areas of necrosis or fibrosis and parenchyma based on enhancement seen on DCEMRI. The average value of these ROIs is reported as ADC of the lesion. The mean number of ROIs used for malignant cases was 20 (range 2–137).

2.5. In vivo ^1H magnetic resonance spectroscopy (MRS) and tCho calculation

Localized single voxel in vivo ^1H MRS was performed after DCEMRI using point resolved spectroscopy (PRESS) pulse sequence. A voxel was positioned within the tumor region avoiding the necrotic areas using reference MR images in three planes i.e., axial, sagittal and coronal. The voxel size was dependent on the tumor volume and it ranged from $10 \times 10 \times 10\ mm^3$ to $10 \times 35 \times 45\ mm^3$. The parameters used with PRESS pulse sequence were: TR = 1500 ms; TE = 100 ms; dummy averages = 8; averages = 128; spectral width = 1000 Hz; vector size = 1024; with a total acquisition time of 3.18 min. Dummy averages were included to obtain steady state magnetization. At long TE though the signal intensity for tCho is less, but enhances its detection by reducing the intense contribution from lipid signals [13,14]. Thus, long echo times (≥100 ms) have been recommended for improved visibility of tCho signal in breast MRS [13–15]. Voxel level manual shimming was carried out for each patient and the line-width of the water resonance ranged from 8 to 20 Hz. A frequency-selective pre-saturation pulse for water suppression was used with water bandwidth of 50 Hz. Spectral lipid suppression was achieved using a bandwidth of 1.8 ppm with the start and end frequencies for the fat region are at 2.2 ppm and 0.4 ppm, respectively.

A spectrum without water and lipid suppression from the same voxel was acquired with a TR of 2000 ms, an echo time of 100 ms with the dummy average = 1 and number of average = 1. For tCho concentration calculation, the internal water signal was used as reference using the formula of Bolan et al. at 4.0 T [16] which was later modified for 1.5 T by Baik et al. [18]. Correction factors were applied to account for T1 and T2 values of water and tCho signal. Baik et al. [18] calculated the T1 and T2 values for Cho and water at 1.5 T (T_1 of Cho = 1500 ms, T_1 of water = 750 ms,T_2 of Cho = 270 ms, and T_2 of water = 97 ms). Substituting these values, the tCho concentration can be calculated as described by us earlier [20] using the equation given below:

$$[Cho] = (I_{Cho} \times 10^{-5}) \times 8792.78\ mmol/kg$$

where (I_{Cho}) is the integral of tCho peak.

Post-processing of spectra was carried out using Syngo GRACE software provided by the manufacturer. The unsuppressed water spectrum was used for both phase and eddy current corrections. For base line correction, a 2.0-Hz line broadening was used with a polynomial order 5.

2.6. Data analyses

The interpretation of DCEMRI data of cytologically/histopathologically proven malignant breast lesions included in this study was carried out based on the types of contrast enhancement curves by an experienced radiologist (SH). The types of curves were defined according to delayed-phase enhancement as persistent, continuing steady increase in signal intensity as type I; plateau, wherein signal intensity does not change in the delayed phase as type II; and type III as washout curves [2,30,31]. According to kinetic analysis, malignant breast lesions with type I and II curves were designated as indeterminate DCE findings. A cut-off value of ADC [5] and tCho concentration [20] for the differentiation of malignant and benign lesions reported using receiver operating characteristics (ROC) analysis was used to define the malignancy in the present study. Accordingly, breast lesions that had an ADC value of $\leq 1.23 \times 10^{-3}\ mm^2/s$ [5] were considered as positive for malignancy. The tCho peak was observed in all patients investigated in water + lipid suppressed spectrum and its concentration was calculated as stated earlier [20]. No spectrum was discarded due to poor quality. The lesions that had tCho concentration value ≥2.54 mmol/kg were categorized as positive for malignancy by MRS [20].

Sensitivity of detection of malignancy by individual parameters (DCEMR curve type, ADC and tCho levels) was calculated using curve analysis and cut-off values given above. The combined analysis of DCEMRI, DWI and ^{1}MRS was carried out using the following criteria: breast lesion was considered positive for malignancy (i) if all 3 parameters are positive, (ii) if any two of the three parameters were positive, and (iii) if any one of the parameters was positive [25].

3. Results

Table 1 summarizes the clinical characteristics, AJCC stage, DCE curve type, histopathological sub-types, BI-RADS categories and the receptor status of patients included in this study. Tumor volume was in the range of 2.21 to 341.2 cm^3 (Mean ± SD: 73.7 ± 77.04 cm^3; Median 51.2 cm^3). Breast lesions were classified in BI-RADS categories

Table 1
The clinical characteristics of patients.

Characteristic	Number of patients (n = 56)
Age in years [Mean ± SD; (range)]	42.8 ± 10.6; (19–70)
Tumor volume (range in cm^3)	2.21–341.2
Menopausal status	
Premenopausal	29
Postmenopausal	27
AJCC stage	
IIA	12
IIB	11
IIIA	9
III (B + C)	22
Hormone receptor status	
ER positive	30
ER negative	23
PR positive	26
PR negative	26
Her2neu positive	20
Her2neu negative	31
DCE curve type	
I	1
II	8
III	47
Histology	
IDC	50
IDC + DCIS	3
Papillary carcinoma	1
DCIS + Cribriform	2
BIRADS	
III	1
IV	11
IVb	2
IVc	2
V	28
VI	11

Note. AJJC staging for 2 patients, BIRADS for 1, ER status for 3, PR status for 4, and Her2 neu status for 5 patients was not available.

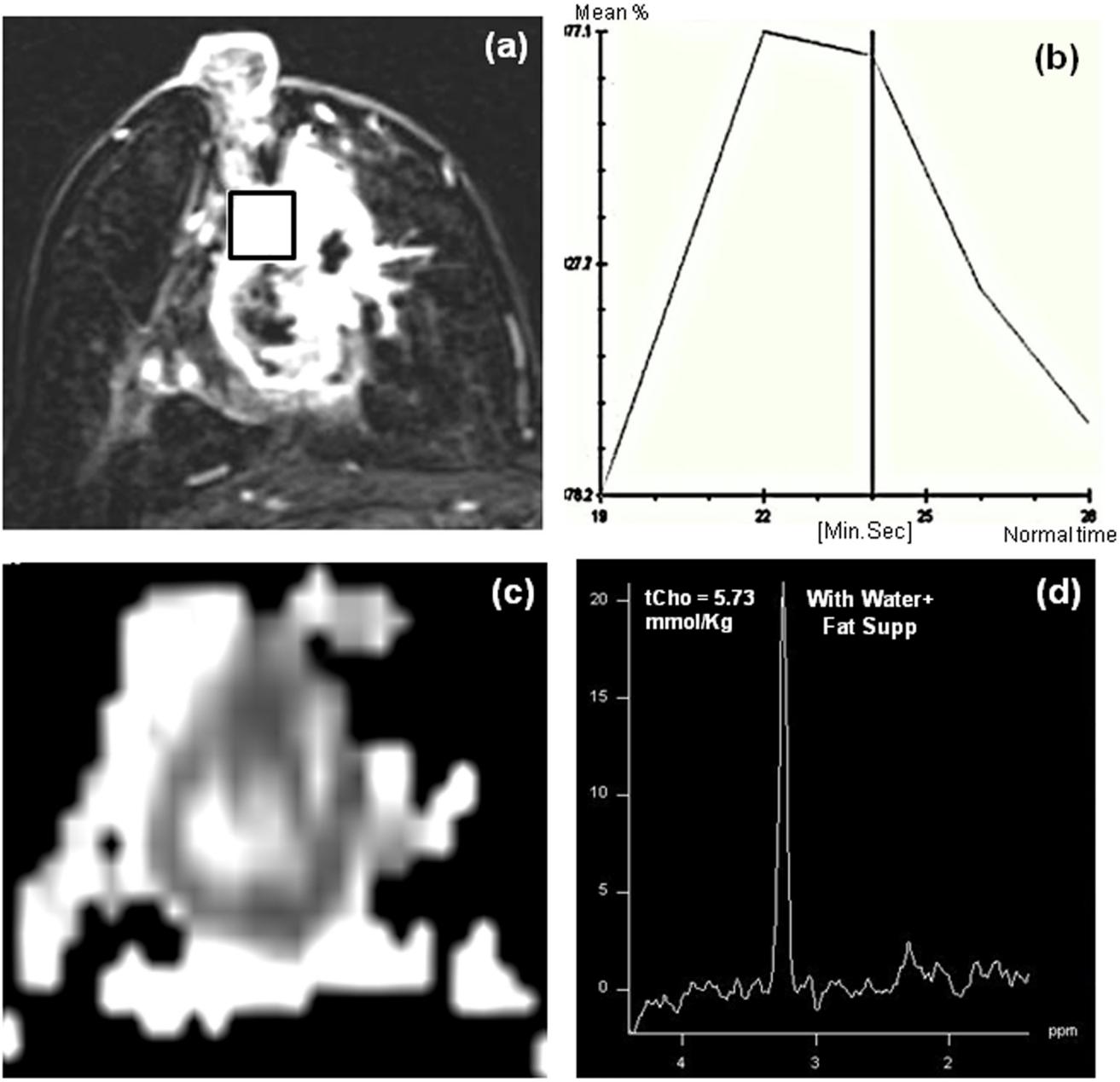

Fig. 1. (a) Representative DCEMR image of a 56-year-old locally advanced breast cancer patient suffering from IDC, and (b) the corresponding type III curve obtained from the ROI positioned on the lesion. (c) shows the ADC map while (d) is the in vivo ^{1}H MR spectrum of the same patient.

based on the evaluation of mammography prior to histopathology and MR imaging as shown in Table 1. The 56 breast lesions were classified as follows: 11 lesions as BI-RADS VI, 28 lesions as BI-RADS V, 11 lesions as BI-RADS IV, 2 lesions as BI-RADS IVb, 2 lesions as BI-RADS IVc and one lesion as BI-RADS III, as shown in Table 1. BI-RADS classification was not available for one lesion. All lesions were proven malignant on cytologically/histopathologically evaluation and the details are as presented in Table 1.

Fig. 1a shows the axial DCEMR image of a 56-year-old patient suffering from infiltrating ductal carcinoma (IDC). The DCEMRI demonstrated a washout pattern of type III as shown in Fig. 1b. The lesion is seen as hypointense area on the ADC map (Fig. 1c) while MRS showed an intense peak due to tCho (Fig. 1d).

Table 2 presents the individual data of histology, AJCC stage, BIRADS, tumor volume, DCE curve type, ADC and tCho for the 14 cases that showed false negative results using either one or two of the parameters. DCEMRI indicated type III curve in 47/56 patients giving a sensitivity of 83.9% for the detection of malignancy. 9/56 patients showed indeterminate DCEMRI findings. Of these, 8 showed type II curve, while one patient had type I curve (Table 3). Histology results revealed 6 cases as IDC and one each as ductal carcinoma in situ, ductal carcinoma in situ + cribriform and papillary carcinoma, respectively.

ADC was below cut-off value (1.23×10^{-3} mm^2/s) for 54/56 cases indicating malignancy thus yielding a sensitivity of 96.4%. DWI was positive for malignancy in all the 9 cases that showed negative findings on DCEMRI [5] (Table 2). However two patients that were positive on DCEMRI with type III curve demonstrated false negative findings on DWI. The histology of these 2 lesions characterized them as IDC.

The tCho concentration was above cut-off value in 50/56 cases, indicating malignancy with a sensitivity of 89.3%. Of the 9 false negative DCEMRI cases, tCho was able to detect malignancy in 6 cases with type II curve. Also, 3 cases that were positive on DCEMRI with

Table 2
Histology, curve type, ADC ($\times 10^{-3}$ mm^2/s), tCho (mmol/kg), AJCC stage and BIRADS of 14 breast cancer patients that had false negative findings either on one or two MR parameters.

S. No.	Patient no	Histology	Curve Type	ADC	tCho	AJCC stage	BIRADS
False negative DCE, true positive ADC and true positive MRS							
1.	7	IDC	II	1.16	3.64	IIB	V
2.	30	IDC	II	0.95	6.78	IIIA	IVb
3.	32	IDC	II	0.98	7.84	IIB	IV
4.	39	Papillary carcinoma	II	1.02	3.62	IIB	V
5.	42	IDC	II	0.97	5.71	IIIB + C	IV
6.	43	IDC	II	0.92	4.3	IIIA	IV
False negative DCE, true positive ADC, false negative MRS							
7.	33	DCIS	I	1.09	1.03	IIB	V
8.	22	DCIS + Cribriform	II	0.97	2.37	IIB	V
9.	41	IDC	II	0.98	2.27	IIA	III
True positive DCE, true positive ADC, false negative MRS							
10.	3	IDC + mucinous carcinoma	III	0.87	2.46	IIB	IV
11.	37	IDC	III	0.98	2.51	IIA	IV
12.	51	IDC	III	1.01	1.35	IIIB + C	VI
True positive DCE, false negative ADC, true positive MRS							
13.	21	IDC	III	1.31	3.45	IIIA	V
14.	49	IDC	III	1.28	4.08	IIIA	V

Note. IDC; infiltrative ductal carcinoma, DCE; dynamic contrast enhanced, ADC; apparent diffusion coefficient, MRS; magnetic resonance spectroscopy; BIRADS; Breast Imaging Reporting and Data System, AJCC; American Joint Committee on Cancer.

Table 3
Sensitivity of DCEMRI, DWI, MRS and multiparametric MRI and number of malignant lesions detected positive by individual and combination of parameters.

Parameter	Sensitivity (%)	True positive	False negative
DCEMRI (curve type)	83.9	47	9
DWI (ADC)	96.4	54	2
MRS (tCho)	89.3	50	6
All 3 of DCEMRI, DWI and MRS	75	42	14
Any 2 of DCEMRI, DWI and MRS	96.4	54	2
Any 1 of DCEMRI, DWI and MRS	100	56	0

type III curve demonstrated false negative findings on MRS (Table 2).

Further, the sensitivity to detect malignancy was calculated using the multi-parametric approach (Table 3). If all 3 MR parameters were considered positive for malignancy then the sensitivity was 75%. While if any two MR parameters were taken as positive, the sensitivity reached to 96.4%. But 100% sensitivity was achieved when anyone of the three parameters was taken as positive for malignancy.

4. Discussion

Multi-parametric MR of using DCEMRI, DWI and MRS provides both functional and molecular information of breast lesions. Several studies have assessed the potential of combining data from DCEMRI and DWI in characterizing breast malignancy [25,26,28,29]. However, only two studies have reported the utility of a combination of multi-parametric approach based on DCEMRI, ADC and MRS in the diagnosis of breast lesions [25,26]. We have earlier documented the potential of ADC in detecting malignancy in indeterminate DCE findings [5]. In the present study, the results of MRS were included into the above data set [5] and evaluated the potential of combination of using DCEMRI, DWI and MRS data in detecting the malignancy in cytologically/histopathologically proven breast cancer cases.

Our results indicated that the sensitivity of detection of malignancy based on DCEMRI was 83.9%, while MRS showed an increased sensitivity of 89.3%. Among the 9 indeterminate DCEMRI cases, MRS detected malignancy in 6 cases. Increased diagnostic accuracy of DCEMRI in combination with ^{1}H MRS have been reported [32,33]. The sensitivity and specificity of ^{1}H MRS for breast malignancy was reported to be in the range of 46 to 100% and between 75 and 100%, respectively [13–25,32–36]. Tozaki et al. [34] showed an increase in the sensitivity of ^{1}H MRS from 44% to 82% after exclusion of lesions of smaller size than 1.5 cm and non-mass lesions with BI-RADS IV and V suggesting that the lesion size was important in detecting tCho using MRS [15,34].

Comparing data from DCEMRI and DWI, of the 56 lesions, 9 were false negative on DCEMRI, however, DWI showed all of them as positive for malignancy when an ADC cutoff of 1.23×10^{-3} mm^2/s was used [5,37,38] This finding demonstrated that the addition of DWI increases the sensitivity (96.4%) and the diagnostic accuracy of breast cancer [25,26,29].

The sensitivity of detection of malignancy was evaluated using multiparametric approach. When all three or any two or any one of the 3 MR parameters were taken as positive for malignancy, then the sensitivities for detecting malignancy were 75%, 96.4% and 100%, respectively. Pinker et al. [26] reported a sensitivity of 100% with an increase in specificity from 64.1 to 87.2% when at least two out of the three techniques yielded positive findings. On the contrary Aribal et al. reported decreased sensitivity and specificity of DCEMRI, DWI and MRS when used in combination than DCEMRI alone [25]. Additionally, Pinker et al. also reported that the accuracy of BI-RADS reading combined with DWI was better than DCEMRI alone [39].

^{1}H MRS can be used as an adjunct modality in clinical practice for cases classified as BI-RADS III and IV [32]. In the present study, MRS and DWI were able to detect malignancy correctly in 4 cases with BI-RADS IV that were false negative on DCEMRI. MRS failed to detect malignancy in a false negative case on DCEMRI with BI-RADS III, however, it was positive on DWI. Thus our study indicated that multiparametric MR approach may be useful in accurate diagnosis of lesions with BI-RADS III and IV.

In this study we used quantitative estimate of absolute concentration of tCho and classified the malignancy based on tCho cut-off value obtained from our earlier study [20] compared to other literature studies [25,26]. Both Aribal et al. [25] and Pinker et al. [26] used only semi-quantitative estimate of tCho for classifying malignancy. In our study, tCho was seen in all 56 lesions. However in 4 false negative findings of MRS, the tCho concentration was in the range of 2.27 to 2.51 mmol/kg, which was marginally lower (1.2 to 10.6%) than the cut-off value used (2.54 mmol/kg). In an earlier study, a tCho cut-off

value of 1.45 mmol/kg was reported for distinguishing benign from malignant lesions [9]. Using this cut-off value, in our cohort 54/56 patients could be categorized as malignant, which yielded a sensitivity of 96.4% for MRS alone.

Further, the 2 false negative cases on DWI had values of ADC in the range of 1.28×10^{-3} mm^2/s to 1.31×10^{-3} mm^2/s which was also only marginally higher (0.8 to 5.0%) than the cut-off value of 1.23×10^{-3} mm^2/s used by us [5,37,38]. A metaanalysis of 13 DWI studies reported that ADC cut-off values for distinguishing malignant and benign lesions was dependent on 'b' values used and it ranged from 1.01×10^{-3} mm^2/s to 1.43×10^{-3} mm^2/s when a 'b' value of 1000 was used [10]. A recent study reported that using an ADC cut-off value of 1.48×10^{-3} mm^2/s, DWI had 88.6% sensitivity and 95.3% specificity for focal lesions of at least 7 mm or above in diameter [12]. Further it was reported that using a cut-off of 1.53×10^{-3} mm^2/s lowered the biopsy rate by 20.9% without affecting the sensitivity [40]. The use of this higher cut-off value categorized all lesions in our patient population as malignant thus increasing the sensitivity of DWI as 100%.

The ROI placement has been reported to significantly influence the measurement of ADC values, also the minimum and the mean ADC values showed better intra- and inter-reader reproducibility [41]. In the present study, the mean ADC was calculated by drawing small circular ROI's encompassing the entire visible tumor on a slice with the largest diameter and avoiding necrotic portions [5]. This approach adopted by us was supported by a recent study wherein it was demonstrated that ADC measurements using small ROI were more accurate than whole region ROI [42]. Thus it may be possible that if DWI and MRS are carried out in a much larger cohort with the use of same methodology of measurements, further refinement in cut-off values can be obtained.

The results of the present study indicated that DCEMRI, DWI and MRS are complementary in the diagnosis of various breast tumor subtypes. The two DCIS lesions which were negative on both DCEMRI [2] and MRS [14] were detected as positive for malignancy by DWI. One papillary carcinoma which was false negative on DCEMRI was detected as positive for malignancy by both DWI and MRS. The IDC lesion with mucinous component was negative on MRS; however it was positive on both DWI and DCEMRI. There are reports in literature that the sensitivity of detection for malignancy was less for MRS in various histological types of breast cancers like DCIS [34], medullary carcinoma [14], mucinous carcinoma [34] and apocrine carcinoma [34]. Kuhl et al. also have reported DCE kinetics to be inconsistent for diagnosis of DCIS lesions [2].

This study has few limitations. Firstly, the inclusion of other types of breast cancers (other than IDC) like DCIS lesions and other histological types are limited. Secondly, the assessment of small lesions by MRS is required. Third is the use of manual ROI for the calculation of ADC, which is subjective and the operator was not blinded to the clinical findings. Also the tumors included in the study were quite large, which reduces its generalizability. For such large lesions, sensitivity is not as important as specificity.

Till date, the various studies presented the diagnostic utility of DCEMRI, DWI, MRS and BIRADS; however, the number of MR parameters that can improve the breast cancer diagnosis is still not clear. Additionally, there is scarcity of inclusion of different histological types of malignant lesions in large numbers and also the benign lesions with different histological types. Therefore, it is important to characterize various histological types of malignant and benign lesions using all the three MR parameters to arrive at a protocol that could be included in a clinical setting for increasing the sensitivity and specificity of non-invasive MR methods. Also there is a need to investigate the lesions with smaller size with an aim to establish the clinical utility of these parameters for better patient care.

5. Conclusion

To summarize, the present study demonstrated the capability of increased detection of malignancy using DCEMRI, DWI and MRS in cytopathologically/histopathologically proven breast cancer. With the use of multi-parametric approach based on the combination of three parameters namely, DCE curve analysis, ADC and tCho, an increase in the sensitivity (100%) was observed. The sensitivity to detect malignancy was highest for DWI compared to MRS and DCEMRI. DWI was able to detect malignancy in all indeterminate DCEMRI cases. Thus the results of the present study suggested that DCEMRI, DWI and MRS may complement each other and may play a significant role in establishing the final diagnosis of malignancy. The utility of these parameters in a large cohort of patients, needs to be demonstrated to make the inclusion of these approaches in a clinical setting.

Declaration of Competing Interest

None.

Acknowledgements

Science and Engineering Research Board (SERB), Government of India is acknowledged for financial support (SP/SO/HS-80/2006 and SR/SO/HS/213/2012) and J.C. Bose Fellowship to NRJ. KA acknowledges the Indian Council of Medical Research, New Delhi for Senior Research Fellowship [3/2/2/241/2014/NCD-III (OPA-31710)].

References

[1] Jemal A, Siegel R, Xu J, Ward E. Cancer statistics. CA Cancer J Clin 2010;60:277–300. [Erratum in: CA Cancer J Clin 2011;61:133-4].
[2] Kuhl C. The current status of breast MR imaging. Part I. choice of technique, image interpretation, diagnostic accuracy, and transfer to clinical practice. Radiology 2007;244:356–78.
[3] Baltzer PA, Benndorf M, Dietzel M, Gajda M, Runnebaum IB, Kaiser WA. False-positive findings at contrast-enhanced breast MRI: a BI-RADS descriptor study. AJR Am J Roentgenol 2010;194:1658–63.
[4] Woodhams R, Ramadan S, Stanwell P, Sakamoto S, Hata H, Ozaki M, et al. Diffusion-weighted imaging of the breast: principles and clinical applications. Radiographics 2011;31:1059–84.
[5] Sharma U, Sah RG, Agarwal K, Parshad R, Seenu V, Mathur SR, et al. Potential of diffusion-weighted imaging in the characterization of malignant, benign, and healthy breast tissues and molecular subtypes of breast Cancer. Front Oncol 2016;6:126.
[6] Sharma U, Jagannathan NR. Characterization of breast tissues by diffusion weighted MR imaging. Biomedical Spectroscopy and Imaging 2014;3:1–13.
[7] Anderson AW, Xie J, Pizzonia J, Bronen RA, Spencer DD, Gore JC. Effects of cell volume fraction changes on apparent diffusion in human cells. Magn Reson Imaging 2000;18:689–95.
[8] Guo Y, Cai YQ, Cai ZL, Gao YG, An NY, Ma L, et al. Differentiation of clinically benign and malignant breast lesions using diffusion-weighted imaging. Magn Reson Imaging 2002;16:172–8.
[9] Rahbar H, Partridge SC. Multiparametric MR imaging of breast Cancer. Magn Reson Imaging Clin N Am 2016;24:223–38.
[10] Chen X, Li WL, Zhang YL, Wu Q, Guo YM, Bai ZL. Meta-analysis of quantitative diffusion-weighted MR imaging in the differential diagnosis of breast lesions. BMC Cancer 2010;29:693.
[11] Zhang L, Tang M, Min Z, Lu J, Lei X, Zhang X. Accuracy of combined dynamic contrast-enhanced magnetic resonance imaging and diffusion-weighted imaging for breast cancer detection: a meta-analysis. Acta Radiol 2016;57:651–60.
[12] Fornasa F, Pinali L, Gasparini A, Toniolli E, Montemezzi S. Diffusion-weighted magnetic resonance imaging in focal breast lesions: analysis of 78 cases with pathological correlation. Radiol Med 2011;116:264–75.
[13] Roebuck JR, Cecil KM, Schnall MD, Lenkinski RE. Human breast lesions: human breast lesions: characterization with proton MR spectroscopy. Radiology 1998;209:269–75.
[14] Yeung DK, Yang WT, Tse GM. Breast Cancer: in vivo proton MR spectroscopy in the characterization of histopathologic subtypes and preliminary observations in axillary node metastases. Radiology 2002;225:190–7.
[15] Katz-Brull R, Lavin PT, Lenkinski RE. Clinical utility of proton magnetic resonance spectroscopy in characterizing breast lesions. J Natl Cancer Inst 2002;94:1197–203.
[16] Bolan PJ, Meisamy S, Baker EH, Lin J, Emory T, Nelson M, et al. In vivo quantification of choline compounds in the breast with ^{1}H MR spectroscopy. Magn Reson Med 2003;50:1134–43.
[17] Meisamy S, Bolan PJ, Baker EH, Pollema MG, Le CT, Kelcz F, et al. Adding in vivo quantitative ^{1}H MR spectroscopy to improve diagnostic accuracy of breast MR imaging: preliminary results of observer performance study at 4.0 T. Radiology 2005;236:465–75.
[18] Baik HM, Su MY, Yu HJ, Mehta R, Nalcioglu O. Quantification of choline containing

compounds in malignant breast tumors by ^{1}H MR spectroscopy using water as an internal reference at 1.5 T. MAGMA 2006;19:96–104.
[19] Haddadin IS, McIntosh A, Meisamy S, Corum C, Styczynski Snyder AL, Powell NJ, et al. Metabolite quantification and high-field MRS in breast cancer. NMR Biomed 2009;22:65–76.
[20] Sah RG, Sharma U, Parshad R, Seenu V, Mathur SR, Jagannathan NR. Association of estrogen receptor, progesterone receptor, and human epidermal growth factor receptor 2 status with total choline concentration and tumor volume in breast cancer patients: an MRI and in vivo proton MRS study. Magn Reson Med 2012;68:1039–47.
[21] Sharma U, Jagannathan NR. MRS in breast Cancer. In: Bottomley PA, Griffiths JR, editors. Handbook of magnetic resonance spectroscopy in vivo: MRS theory, practice and applications. Chichester, UK: John Wiley & Sons Ltd; 2015. p. 981–95. Online edition in: eMagRes. [4:821-832].
[22] Klomp DW, van de Bank BL, Raaijmakers A, Korteweg MA, Possanzini C, Boer VO, et al. ^{31}P MRSI and ^{1}H MRS at 7 T: initial results in human breast cancer. NMR Biomed 2011;24:1337–42.
[23] Ramazan A, Demircioglu O, Ugurlu U, Kaya H, Aribal E. Efficacy of single voxel ^{1}H MR spectroscopic imaging at 3T for the differentiation of benign and malignant breast lesions. Clin Imaging 2016;40:831–6.
[24] Montemezzi S, Cavedon C, Camera L, Meliadò G, Caumo F, Baglio I, et al. ^{1}H MR spectroscopy of suspicious breast mass lesions at 3T: a clinical experience. Radiol Med 2017;122:161–70.
[25] Aribal E, Asadov R, Ramazan A, Ugurlu MÜ, Kaya H. Multiparametric breast MRI with 3T: effectivity of combination of contrast enhanced MRI, DWI and ^{1}H single voxel spectroscopy in differentiation of breast tumors. Eur J Radiol 2016;85:979–86.
[26] Pinker K, Bogner W, Baltzer P, Gruber S, Bickel H, Brueck B, et al. Improved diagnostic accuracy with multiparametric magnetic resonance imaging of the breast using dynamic contrast-enhanced magnetic resonance imaging, diffusion-weighted imaging, and 3-dimensional proton magnetic resonance spectroscopic imaging. Investig Radiol 2014;49:421–30.
[27] Aboagye EO, Bhujwalla ZM. Malignant transformation alters membrane choline phospholipid metabolism of human mammary epithelial cells. Cancer Res 1999;59:80–4.
[28] . Kul S, Cansu A, Alhan E, Dinc H, Gunes G, Reis A. Contribution of diffusion-weighted imaging to dynamic contrast-enhanced MRI in the characterization of breast tumors. AJR Am J Roentgenol 201;196:210–7.
[29] Pinker K, Baltzer P, Bogner W, Leithner D, Trattnig S, Zaric O, et al. Multiparametric MR imaging with high-resolution dynamic contrast-enhanced and diffusion-weighted imaging at 7 T improves the assessment of breast tumors: a feasibility study. Radiology 2015;276:360–70.
[30] Kuhl CK, Mielcareck P, Klaschik S, et al. Dynamic breast MR imaging: are signal intensity time course data useful for differential diagnosis of enhancing lesions? Radiology 1999;211:101–10.
[31] Orel SG. Differentiating benign from malignant enhancing lesions identified at MR imaging of the breast: are time-signal intensity curves an accurate predictor? Radiology 1999;211:5–7.
[32] Vassiou K, Tsougos I, Kousi E, Vlychou M, Athanasiou E, Theodorou K, et al. Application value of 3T ^{1}H-magnetic resonance spectroscopy in diagnosing breast tumors. Acta Radiol 2013;54:380–8.
[33] Lipnick S, Liu X, Sayre J, Bassett LW, Debruhl N, Thomas MA. Combined DCE-MRI and single-voxel 2D MRS for differentiation between benign and malignant breast lesions. NMR Biomed 2010;23:922–30.
[34] Tozaki M, Fukuma E. ^{1}H MR spectroscopy and diffusion-weighted imaging of the breast: are they useful tools for characterizing breast lesions before biopsy? AJR Am J Roentgenol 2009;193:840–9.
[35] Begley JK, Redpath TW, Bolan PJ, Gilbert FJ. In vivo proton magnetic resonance spectroscopy of breast cancer: a review of the literature. Breast Cancer Res 2012;14:207.
[36] Tozaki M, Hoshi K. ^{1}H MR spectroscopy of invasive ductal carcinoma: correlations with FDG PET and histologic prognostic factors. AJR Am J Roentgenol 2010;194:1384–90.
[37] Baltzer PA, Renz DM, Herrmann KH, Dietzel M, Krumbein I, Gajda M, et al. Diffusion-weighted imaging (DWI) in MR mammography (MRM): clinical comparison of echo planar imaging (EPI) and half-Fourier single-shot turbo spin echo (HASTE) diffusion techniques. Eur Radiol 2009;19:1612–20.
[38] Bogner W, Pinker-Domenig K, Bickel H, Chmelik M, Weber M, Helbich TH, et al. Readout-segmented echo-planar imaging improves the diagnostic performance of diffusion-weighted MR breast examinations at 3.0 T. Radiology 2012;263:64–76.
[39] Pinker K, Bickel H, Helbich TH, Gruber S, Dubsky P, Pluschnig U, et al. Combined contrast-enhanced magnetic resonance and diffusion-weighted imaging reading adapted to the "breast imaging reporting and data system" for multiparametric 3-T imaging of breast lesions. Eur Radiol 2013;23:1791–802.
[40] Rahbar H, Zhang Z, Chenevert TL, Romanoff J, Kitsch AE, Hanna LG, et al. Utility of diffusion-weighted imaging to decrease unnecessary biopsies prompted by breast MRI: a trial of the ECOG-ACRIN Cancer research group (A6702). Clin Cancer Res 2019;25:1756–65.
[41] Bickel H, Pinker K, Polanec S, Magometschnigg H, Wengert G, Spick C, et al. Diffusion-weighted imaging of breast lesions: region-of-interest placement and different ADC parameters influence apparent diffusion coefficient values. Eur Radiol 2017;27:1883–92.
[42] Arponen O, Sudah M, Masarwah A, Taina M, Rautiainen S, Könönen M, et al. Diffusion-weighted imaging in 3.0 tesla breast MRI: diagnostic performance and tumor characterization using small subregions vs. whole tumor regions of interest. PLoS One 2015;10:e0138702. doi: 10.1371/journal.pone.0138702 and e0141833 https://doi.org/10.1371/journal.pone.0141833.